

SCIENTIFIC DATA

OPEN Data Descriptor: Survival, gene and metabolite responses of *Litoria verreauxii alpina* frogs to fungal disease chytridiomycosis

Received: 31 August 2017

Accepted: 8 January 2018

Published: 6 March 2018

Laura F. Grogan^{1,2,3}, Jason Mulvenna^{3,4}, Joel P. A. Gummer^{5,6}, Ben C. Scheele^{2,7}, Lee Berger², Scott D. Cashins², Michael S. McFadden⁸, Peter Harlow⁸, David A. Hunter⁹, Robert D. Trengove^{5,6} & Lee F. Skerratt²

The fungal skin disease chytridiomycosis has caused the devastating decline and extinction of hundreds of amphibian species globally, yet the potential for evolving resistance, and the underlying pathophysiological mechanisms remain poorly understood. We exposed 406 naïve, captive-raised alpine tree frogs (*Litoria verreauxii alpina*) from multiple populations (one evolutionarily naïve to chytridiomycosis) to the aetiological agent *Batrachochytrium dendrobatidis* in two concurrent and controlled infection experiments. We investigated (A) survival outcomes and clinical pathogen burdens between populations and clutches, and (B) individual host tissue responses to chytridiomycosis. Here we present multiple interrelated datasets associated with these exposure experiments, including animal signalment, survival and pathogen burden of 355 animals from Experiment A, and the following datasets related to 61 animals from Experiment B: animal signalment and pathogen burden; raw RNA-Seq reads from skin, liver and spleen tissues; *de novo* assembled transcriptomes for each tissue type; raw gene expression data; annotation data for each gene; and raw metabolite expression data from skin and liver tissues. These data provide an extensive baseline for future analyses.

Design Type(s)	randomized complete block design • pathogenicity design
Measurement Type(s)	susceptibility to infectious agent • transcription profiling • metabolite profiling
Technology Type(s)	real time polymerase chain reaction assay • RNA sequencing • mass spectrometry assay
Factor Type(s)	host exposure to environment containing infectious agent • geographic location • pathogen challenge • biological replicate • animal body part
Sample Characteristic(s)	<i>Litoria verreauxii</i> • liver • New South Wales • skin of body • spleen • skin mucus

¹Griffith Wildlife Disease Ecology Group, Environmental Futures Research Institute and School of Environment, Griffith University, Nathan, Queensland 4111, Australia. ²One Health Research Group, College of Public Health, Medical and Veterinary Sciences, James Cook University, Angus Smith Drive, Townsville, Queensland 4811, Australia. ³Genetics and Computational Biology, QIMR Berghofer Medical Research Institute, 300 Herston Road, Brisbane, Queensland 4006, Australia. ⁴School of Biomedical Sciences, The University of Queensland, Brisbane, Queensland 4072, Australia. ⁵Separation Science and Metabolomics Laboratory, Murdoch University, Perth, Western Australia 6150, Australia. ⁶Metabolomics Australia, Murdoch University Node, Murdoch University, Perth, Western Australia 6150, Australia. ⁷Fenner School of Environment and Society, Australian National University, Canberra, Australian Capital Territory 2601, Australia. ⁸Taronga Conservation Society Australia, Bradleys Head Road, Mosman, New South Wales 2088, Australia. ⁹Ecosystems and Threatened Species, South West Region, NSW Office of Environment and Heritage, Albury, New South Wales 2640, Australia. Correspondence and requests for materials should be addressed to L.F.G. (email: l.grogan@griffith.edu.au).

Background & Summary

Over one third of all amphibian species around the world are threatened with extinction¹. One of the main causes of declines is the spread of the lethal skin disease chytridiomycosis, caused by the fungal pathogen *Batrachochytrium dendrobatidis* (Bd)^{2–4}. Despite considerable research in recent decades, methods for disease mitigation *in situ* are still in their infancy⁵. Accelerated evolution of disease resistance via marker-assisted selection may provide a long-term management solution for species at continued risk of decline^{6,7}. Such evolution of disease resistance has been demonstrated in natural disease systems^{8,9}, and marker-assisted selection has been widely utilized in domestic animals and agriculture^{10,11}.

The mechanisms underpinning chytridiomycosis pathophysiology and the potential for the evolution of host resistance are currently poorly understood¹². This is partly because as yet there is no clear, controlled example of the evolution of host resistance to chytridiomycosis which would enable investigation of evolving mechanisms of resistance. One way to test for evolution of resistance without undertaking logistically infeasible longitudinal studies is by comparing the survival of experimentally challenged frogs between exposed populations and geographically-related Bd-naïve populations. Geographic proximity acts to control for other evolutionary forces by providing ecological similarity other than the presence of chytridiomycosis.

The alpine tree frog (*Litoria verreauxii alpina*), an endangered and highly Bd-susceptible subspecies endemic to the sub-alpine regions of Victoria and New South Wales in south-eastern Australia provided us with a unique opportunity to explore this question of the potential for evolution of host resistance. Throughout its range, *L. v. alpina* experienced major declines from the early 1980s when Bd is believed to have arrived¹³, resulting in the extirpation of most known populations^{14,15}. However, we were aware of one population (Grey Mare in Kosciuszko National Park, Australia; Fig. 1) that by virtue of relative geographic isolation had hitherto eluded disease emergence.

We thus collected multiple clutches of eggs from this infection-naïve population in 2010, plus three other exposed populations (first exposed to Bd approximately 26 years earlier based on unpublished reports of declines) and raised the frogs in captivity. The naïve population, Grey Mare, remained uninfected until late in 2012, when the arrival of Bd at this site had a catastrophic effect, with few frogs observed since (B. Scheele unpublished data). A small number of remaining *L. v. alpina* populations now persist despite high ongoing annual adult mortality associated with chytridiomycosis^{13,15}. Multiple studies have been performed on *L. v. alpina* at these study sites, providing a comprehensive background of ecological and disease dynamic information^{13,15–20}.

In this study we examined clinical host susceptibility (survival and infection intensity), and underlying gene expression and metabolomics responses of key host tissues to compare the immunology and

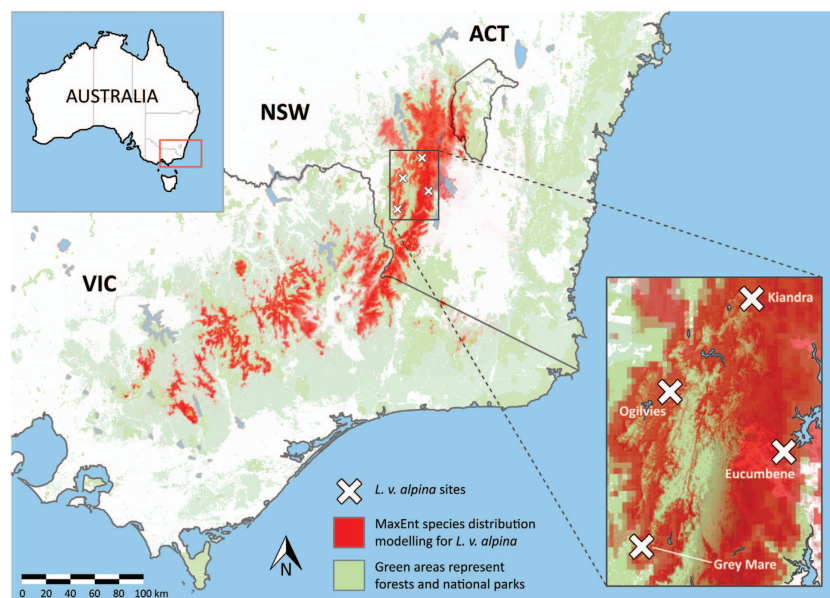


Figure 1. Map demonstrating location of the four source populations of *L. v. alpina* used in this study. Inset shows greater detail. Red shading represents the predicted distribution range of *L. v. alpina*, using species distribution modelling algorithm MaxEnt and species presence data sourced from the Atlas of Living Australia (ALA) and filtered according to expert knowledge of subspecies distributions^{41–45}. Green shading represents state forests and national parks. The effects of chytridiomycosis on the distribution of *L. v. alpina* have not been incorporated.

Population (total number frogs) [*]	Clutch (total number frogs) [*]	Exposure group [†]	Total number of frogs	Number of males [‡]	Number of females [‡]	Number with undetermined gender
Eucumbene (99)	A (30)	E	20	7	13	0
		C	10	6	4	0
	B (19)	E	19	10	9	0
		C	0	0	0	0
	C (29)	E	20	10	10	0
		C	9	4	5	0
D (21)	E	E	19	11	8	0
		C	2 [§]	0	1	1
	C					
Grey Mare (80)	A (14)	E	14	7	6	1
		C	0	0	0	0
	B (26)	E	20	10	10	0
		C	6	3	3	0
	C (29)	E	20	11	9	0
		C	9	6	3	0
	D (11)	E	11	9	2	0
		C	0	0	0	0
Kiandra (100)	A (25)	E	20	9	11	0
		C	5	1	4	0
	B (25)	E	20	12	8	0
		C	5	1	4	0
	C (25)	E	20	8	10	2
		C	5	3	2	0
	D (25)	E	20	11	9	0
		C	5	1	4	0
Ogilvies (76)	A (19)	E	19	13	6	0
		C	0	0	0	0
	B (40)	E	20	7	13	0
		C	20	6	14	0
	C (17)	E	16	9	7	0
		C	1 [¶]	0	0	1

Table 1. Experimental design for *L. v. alpina* clinical survival experiment, Experiment A. Numbers of *L. v. alpina* frogs from each population and clutch are outlined, including details of blind randomized block design used for allocation of treatment groups (exposed frogs versus sham-exposed negative control frogs).

*Total number of frogs in parentheses for each group. †E represents exposed frogs, C represents control frogs.

‡Gender as determined by post-mortem coelomic examination. §Includes one frog that died

pre-exposure and was excluded from data records. ||This number includes a frog that died of anasarca

post-exposure, unrelated to chytridiomycosis, data still included (frog ID: Lva162). ¶This frog died

pre-exposure and was excluded from data records.

pathophysiology of infection between populations. Our aim was to investigate whether persisting long-exposed populations may have evolved disease resistance compared with the naïve population, and to characterize potentially resistant phenotypes. We performed two related experiments on a total of 406 adult *L. v. alpina* via controlled laboratory Bd-exposure. The specific aims of our experiments and data collection were to (1) examine associations between survival, infection burden, and tissue immune and physiologic responses (via measurement of gene expression and metabolite accumulation) within individuals, clutches, and populations of frogs, (2) compare population responses between naïve and long-exposed populations, and (3) compare infection responses at various times post exposure, with a focus on the subclinical infection stage.

The specific data we collected included animal signalment, survival, pathogen burden, raw RNA-Seq reads from skin, liver and spleen tissues, *de novo* assembled transcriptomes for each tissue type, raw gene expression data, annotation data for each gene, and raw metabolite expression data from skin and liver tissues. Tables 1 and 2 provide a quantitative overview of the numbers of frogs, their source populations, clutches and respective treatments in the exposure experiment. Table 3 (available online only) provides

Populations	Exposure – Day 0	Day 4	Day 8	Day 14
	Total # exposed	# exposed sampled	# exposed sampled	# exposed sampled
	(total # control)*	(# control sampled) [†]	(# control sampled) [†]	(# control sampled) [†]
Grey Mare (clutch B)	12 (3)	4 (1)	4 (1)	4 (1)
Eucumbene (clutch D)	12 (6)	4 (2)	4 (2)	4 (2)
Kiandra (clutch B)	12 (6)	4 (2)	4 (2)	4 (2)
Total	36 (15)	12 (5)	12 (5)	12 (5)

Table 2. Experimental design for *L. v. alpina* tissue response experiment, Experiment B. Numbers of frogs from each population and treatment group (Bd exposed or unexposed control) sampled at each time point post exposure are indicated. The 10 frogs from Experiment A that demonstrated clinical signs are excluded from this table (as their sampling date was contingent on infection progression). *Total number of unexposed control frogs shown in parentheses [†]Number of unexposed control frogs sampled shown in parentheses.

summary descriptions of the data associated with this manuscript. Figure 2 provides a schematic overview of the steps involved in transcriptomic analysis and the corresponding data outputs. These data have already been used to examine gene associations with survival¹⁶, differential gene expression²¹ and metabolite accumulation (L. Grogan unpublished data). Additional analyses could include (1) the investigation of specific genes or gene groups of interest, identified using sequence information provided by transcriptome assembly, (2) the examination of gene and isoform variation between populations, and (3) the determination of novel or common mechanisms of resistance/susceptibility amongst other well characterised disease systems.

Methods

Animals were sourced as infection-naïve eggs from four wild populations

Up to four clutches of alpine tree frog eggs (*Litoria verreauxii alpina*) with unknown but possible multiple paternity were collected by D. Hunter in 2010 from each of four ecologically similar but geographically distinct wild populations from around Kosciuszko National Park, New South Wales, Australia, in accordance with Scientific Licence number S12848 (total of 15 clutches). The source populations are hereafter designated Kiandra (35.872°S 148.500°E 1356 m above sea level [asl]), Eucumbene (36.152°S 148.563°E 1451 m asl), Grey Mare (36.317°S 148.260°E 1525 m asl), and Ogilvies (36.036°S 148.322°E 1307 m asl) (Fig. 1). Detailed descriptions of the sites can be found in Scheele et al. (2015)¹⁵. Three of the four populations (Kiandra, Eucumbene and Ogilvies) had a multi-generational history (over two decades) of exposure to the fungal pathogen Bd^{13,14}. The remaining population (Grey Mare) was at the time evolutionarily naïve to the pathogen due to relative geographic isolation, until the pathogen's emergence there in 2012 (B. Scheele unpublished data).

Captive husbandry was performed under quarantine conditions

Animals were captive-reared in clutch groups at Taronga Zoo, Sydney, Australia, until approximately eight months post-metamorphosis (in 2011). Experienced animal handlers followed routine rearing protocols under quarantine conditions in accordance with guidelines approved by Taronga Conservation Society Animal Ethics Committee (4c/01/10). Adult frogs were transferred to individual enclosures several weeks prior to commencement of the infection exposure experiment to allow for acclimatization to enclosures and conditions. From this time, frogs were maintained at constant 19 °C (±2 °C) in individual plastic containers with permeable gauze lids, pebble substrate, and water drainage holes down one end of the tub. Enclosures were placed at a slight angle (10°) to facilitate water drainage and provide wet and dry areas. Frogs were fed multivitamin and calcium-dusted crickets alternately twice weekly *ad libitum*. Individual frogs were observed daily by an experienced animal handler and veterinarian for examination of health status and clinical signs of disease. A small hand-held hose was used to flush tubs daily via the gauze top of the tub. Tubers were flushed for at least 15 s with filtered water until the water ran clear and debris was removed.

Experimental design involved blinded, randomized and controlled treatment groups

Experimental protocols involving animals were carried out in accordance with the approved guidelines and protocols under permits issued by James Cook University (A1408) and Taronga Conservation Society (4c/01/10) Animal Ethics Committees. From among the captive-reared *L. v. alpina*, a total of 406 chytridiomycosis-naïve adult frogs were prepared for the exposure experiment. The number of frogs available for utilization was subject to original clutch size and natural attrition during growth and development. An unexposed negative control group was randomly assigned to control for experimental effects, and operators were blinded to treatment groups. We maximized the sample size of exposed frogs for experimental purposes by randomly selecting up to 20 frogs from each block (blocks consisted of

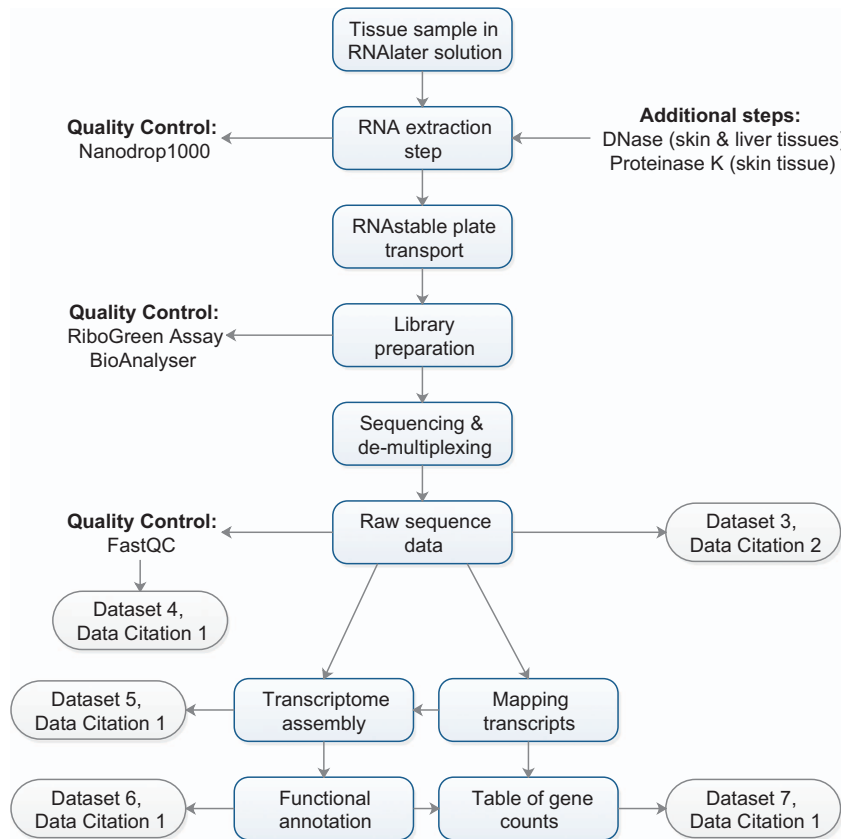


Figure 2. Schematic overview of the transcriptomic analyses performed in the study, and the corresponding quality control measures and data outputs.

Three tissues were collected from each frog ($n = 61$) for transcriptomic analysis, yielding a total of $n = 181$ samples (2 missing data). All tissue samples underwent RNA extraction, however skin and liver samples had their total RNA extracted with 5-Prime PerfectPure kit and were subject to a DNase step, skin samples were subject to a Proteinase K step, and spleen samples had their RNA extracted with Qiagen RNeasy minikit. All RNA samples were subject to quality control steps, library preparation and sequencing, producing raw sequence data for each sample. Tissue-specific transcriptomes were assembled *de novo* with Trinity³⁴ and functionally annotated with BLAST2GO³⁶ (with inbuilt quality control measures, including minimum e-value and percentage similarity), and henceforth all sample data were aligned and annotated based on these.

specific clutches, A-D, within the four populations) to be exposed to Bd. Some clutches were of insufficient sample size to permit the allocation of negative control individuals (Eucumbene clutch B, Grey Mare clutches A and D, Ogilvies clutches A and C).

We needed to run two concurrent experiments under identical conditions in order to link survival results (Experiment A) with tissue-level responses (Experiment B). This experimental design was necessary because animals had to be sacrificed during the course of infection in Experiment B in order to obtain tissues. Our experimental design accommodated for this purpose by using siblings across both experiments that were collected from the same wild egg clutches (with possible multiple-paternity).

Experiment A—Survival experiment. Experiment A utilized 355 frogs in a clinical survival experiment and involved random allocation of frogs from all populations and clutches, according to a controlled, randomized, stratified block design outlined in Table 1.

Experiment B—Tissue response experiment. Experiment B utilized 51 frogs independent of those in Experiment A, plus an additional 10 frogs from Experiment A that were sampled upon euthanasia when showing clinical signs of chytridiomycosis. The dual use of the 10 frogs from Experiment A allowed us to reduce the total number of frogs used for ethical reasons while improving statistical power. The purpose of Experiment B was to investigate underlying immune and pathophysiological responses to infection. Frogs were randomly selected from specific clutches (corresponding to clutches also used in the survival experiment) and humanely euthanized for tissue sampling at various time points post-exposure. This

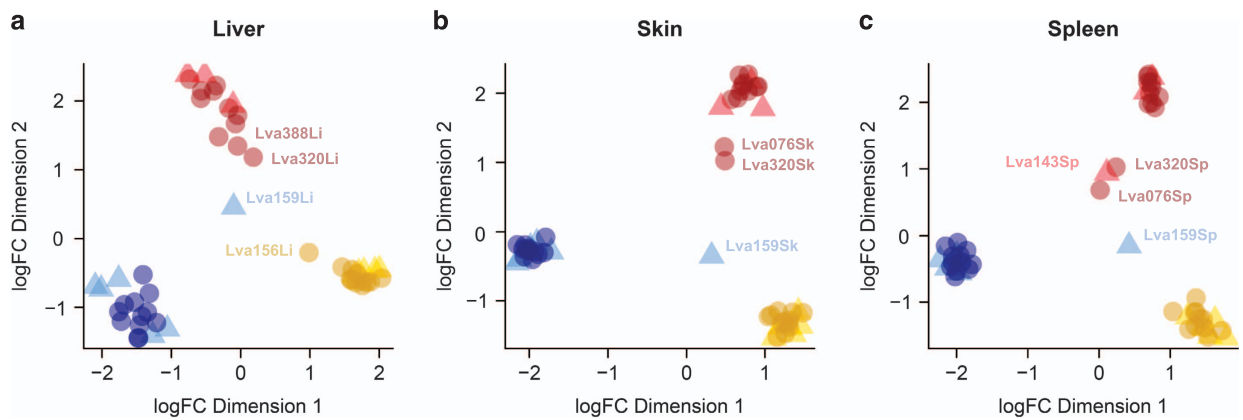


Figure 3. Unsupervised classical (metric) multi-dimensional scaling plots (using plotMDS and recommended settings from the Bioconductor package EdgeR) demonstrating leading log-fold differences in gene expression results between pairs of samples. Uninfected negative control frog samples (\blacktriangle), Bd-exposed frog samples (\bullet). Samples predominantly cluster by source population (colour groups: Eucumbene—blue, Grey Mare—red, and Kiandra—yellow). (a) Liver samples, (b) skin samples, and (c) spleen samples. Visually identified group outliers have been labeled with frog and tissue ID for ease of comparison (they were not removed from analyses). Reprinted with permission from Grogan et al. (2018)²¹.

experiment involved 18 frogs from each of Eucumbene (Clutch D) and Kiandra (Clutch B) populations (including 6 negative control animals from each population), and 15 frogs from Grey Mare (Clutch B) (including 3 negative control animals; Table 2), plus the additional 10 frogs from Experiment A (4 frogs from Grey Mare, and 2 each from the remaining 3 populations). Our study design resulted in 3 to 4 biological replicates per group at the lowest level of comparison (comparing gene and metabolite expression from each population and sampling time post exposure; as commonly utilized in transcriptomics studies), and higher numbers in the pooled group comparisons (comparing populations, or sampling times post exposure). In order to examine for batch effects, we sampled control frogs from across all sampling sessions rather than within a single session. Initial clutch sizes were limiting in some cases, leading to a lower overall number of frogs available (particularly regarding the number of control frogs from Grey Mare).

Frogs were exposed to Bd or sham-exposed to DSS

A Bd strain (AbercrombieNP-L.booroolongensis-09-LB-P7), isolated in May 2009 from a healthy adult frog and minimally passaged (from Abercrombie River National Park, a site roughly 230 km north-east of the study sites), was used for inoculations on 20th September, 2011. All Australian isolates examined thus far have been identified to belong to the hypervirulent global panzootic lineage (Bd-GPL^{6,22}). The strain was maintained and infectious zoospores collected and counted as described previously²³. In brief, we cultured Bd at 20 °C on mTGH agar plates (8 g L⁻¹ tryptone, 2 g L⁻¹ gelatin hydrolysate, 4 g L⁻¹ lactose, 10 g L⁻¹ agar, with the addition of 200 mg L⁻¹ penicillin-G and 200–500 mg L⁻¹ streptomycin sulfate) before flooding plates with 10 mL dilute salts solution (DSS: 1.0 mMol KH₂PO₄, 0.2 mMol CaCl₂·H₂O, 0.1 mMol MgCl₂·2H₂O) for 20 min. Zoospore concentration was determined using a haemocytometer and dilutions were adjusted for consistency.

Frogs were confirmed negative to Bd (via qPCR, see below) prior to the commencement of the exposure experiment, and assigned an identification number (Lva001-Lva406) randomly with respect to population, clutch and treatment group. Two frogs died during the acclimatization period pre-exposure (Lva209 and Lva303), and another frog died post-exposure from a condition unrelated to chytridiomycosis (anasarca and cloacal prolapse; Lva162). Data from the former two frogs is not included, leaving a total of 404 experimental animals (details in Table 1). A total of 278 frogs from Experiment A (including the 10 crossed-over to Experiment B), and 36 frogs from Experiment B were individually exposed to 750,000 zoospores in 25 mL DSS, with enclosures held flat without pebble substrate for 18 h. Following exposure, enclosures were held horizontally for a further two days, however, the water was replaced daily, before having pebbles added and being placed again on a mild angle (10°) for ease of drainage. Seventy-five negative control frogs from Experiment A and 15 from Experiment B were subject to identical conditions, but were instead sham-exposed with only DSS.

Animal discomfort was minimized, and individual frogs were observed daily by an experienced animal handler and/or veterinarian for health status. If clinical signs of chytridiomycosis infection were detected (dullness, lethargy, peripheral erythema and increased skin shedding), the frog was immediately humanely euthanized using an overdose of a concentrated buffered anaesthetic agent tricaine methanesulfonate (MS-222). Survival data (date of death), measurement data (mass, snout-urostyle

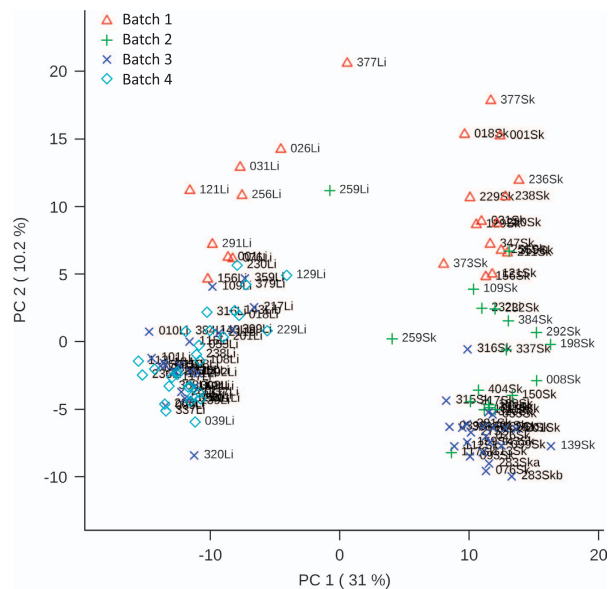


Figure 4. Principal components analysis scores plot for metabolite expression from both liver and skin tissue samples (L. Grogan unpublished data). Expression data was first normalized by Total Area under Chromatogram by sample, and overall dataset log transformation and pareto scaling. Samples separate by tissue type on the horizontal axis (Principal Component 1, representing 31% of the variability) with liver samples on the left ('Li' in sample name) and skin samples on the right ('Sk' in sample name). Samples separate only mildly by batch (date of processing) on the vertical axis (Principal Component 2, representing 10.2% of the variability), consistent with preventative GC-MS maintenance regimens.

length, sex), and skin swabs for Bd infection intensity (ascertained via qPCR as described below) were collected for frogs from Experiment A (Dataset 1; Data Citation 1).

Skin, liver and spleen tissues were sampled at specific times post exposure (Experiment B)

Three sampling sessions were performed at 4, 8 and 14 days post exposure (DPE; corresponding with subclinical infections) using a randomized block design (each session sampled a total of 17 animals, including control frogs (stratified by populations of origin; see Table 2 for experimental design). In addition to the 51 frogs already described, 10 exposed frogs were obtained from Experiment A and sampled between 28 and 30 DPE when they began to exhibit clinical signs of chytridiomycosis and were hence in the terminal stages of disease. These additional frogs included two from each of Kiandra, Eucumbene, and Ogilvies populations, and four frogs from Grey Mare. Immediately prior to humane euthanasia (via rapid double pithing, to avoid possible effects of MS-222 on tissue physiology), frogs were examined, weighed, had their snout-urostyle length measured, and were skin swabbed (as described below) to confirm infection status and to quantify Bd infection intensity via qPCR (Dataset 2; Data Citation 1).

Immediately following euthanasia of each frog, a post-mortem examination via ventral midline coeliotomy was performed for collection of tissues for subsequent analyses. Tissues collected included (1) ventral abdominal skin and liver that were immediately transferred to 500 μ L 100% methanol and stored at -80°C , and (2) ventral abdominal and thigh skin, spleen and liver that were immediately transferred to RNeasy (Qiagen, Australia) and refrigerated overnight at 4°C before being stored longer-term at -80°C . The ventral abdominal and thigh skin of frogs are common sites for Bd infection^{2,24}. The spleen is the main peripheral lymphoid or immunological organ of frogs²⁵. The liver is an important organ for many physiological functions including several associated with both immunity and pathogenesis of infectious disease (such as immune surveillance, detoxification of antigens, removal of debris, breakdown of the products of apoptosis, and assimilation of energy²⁶). Sex was ascertained via examination of coelomic reproductive organs and forelimb nuptial pads on males (sexual dimorphism in frogs of this age was not consistently expressed).

Swabs were collected weekly and pre-euthanasia to determine infection intensities via qPCR (Experiment A)

Bd infection intensity data on individual frogs (in zoospore equivalents, ZSE) was obtained by first collecting skin swabs. Swabbing was conducted pre-euthanasia for every frog, as well as weekly for frogs from Experiment A from week two post-exposure onwards, including on the final day of the experiment

for all surviving frogs (15th December, 2011; total experimental length 86 days). Swabbing was conducted under quarantine conditions using new gloves and a new sterile dry swab per frog (MW 100-100; Medical Wire and Equipment, Bath, UK). Swabs were rotated continuously while being drawn along the palmar and plantar surfaces of each of the fore and hind-feet four times, as well as both sides of the ventral abdomen. Swabs were sealed individually and stored dry at 4 °C, or frozen longer-term at -20 °C. A selection of collected swabs from weekly sampling sessions, as well as all pre-euthanasia swabs, were analyzed for Bd DNA in triplicate with the TaqMan real-time qPCR protocol^{27,28}, and each run included an internal positive control. Samples that recorded only one or two of the three wells as a low positive were considered positive to maximise diagnostic sensitivity²⁹.

Transcriptomics methods

RNA extractions. Total RNA was isolated from skin, liver and spleen tissue samples that had been stored in RNAlater following the manufacturer's protocol for 5-Prime PerfectPure RNA Tissue kits (Eppendorf-5 Prime, Boulder, CO, USA) for liver and skin samples and Qiagen RNeasy mini kits for spleen samples (the spleens were considerably smaller in volume and required a more sensitive method). Tissues were first removed from RNAlater and then lysed on ice using a rotor-stator homogenizer. Liver and skin lysates were treated with DNase to remove genomic DNA, and skin lysates were subject to an additional proteinase K step to digest keratin, remove excess proteins, and inactivate nucleases. Pure total RNA was eluted in nuclease-free water. RNA quantity was determined with a Nanodrop 1000 spectrophotometer, the absorption ratios 260/280 (~2.0) and 260/230 (2.0-2.2) were assessed, and the spectral pattern was evaluated in order to determine RNA integrity and purity. RNAsable plates (Biomatrix, California USA) were used to ship total RNA samples dry and at room temperature to Minnesota BioMedical Genomics Centre, USA.

RNA-Seq using the Illumina HiSeq 2000 platform. Total RNA samples were reconstituted with nuclease-free water, quantified with a fluorimetric RiboGreen assay, and had their quality assessed with capillary electrophoresis (Agilent BioAnalyzer 2100; Agilent, Santa Clara, CA, USA). Samples containing >1 µg total RNA and having an RNA Integrity Number (RIN)>8 passed quality control. Copy DNA Illumina sequencing libraries were created from each of the samples following manufacturer specifications (Illumina Truseq RNA Sample Preparation Kit), and up to 12 samples were individually indexed by the ligation of adaptors for multiplexing on each flow cell lane. Indexed libraries were gel-size selected to 320 bp +/- 5%, and hybridized to a paired end flow cell, before being clonally amplified by bridge amplification, and sequenced with the Illumina HiSeq 2000 (Illumina, San Diego, CA). Base call data for paired end reads from each sample were analyzed and de-multiplexed with CASAVA software 1.8.2 (Illumina, San Diego, CA) generating .fastq files for each sample (Data Citation 2).

Transcriptome assembly, annotation, and sample gene abundance quantification. The 100 bp paired end read sequences from each sample were first examined for read quality using FastQC as described under Technical Validation below (Dataset 4; Data Citation 1). Trimmomatic 0.30 (ref. 30) was run in paired end mode to trim TruSeq adapter sequences, crop Illumina's random hexamers³¹, perform sliding window trimming (window size 4, required quality 15), trim low quality bases from each end of reads (required quality 3), and ensure that the minimum length of resultant reads was at least 75 bases. Widowed reads were retained as unpaired forward and reverse read files. We performed digital normalization to reduce overall data set size and remove read redundancy using DigiNorm³² with the -p flag for the paired read files. We then used Bowtie³³ to remove reads aligning to the Bd genome. The remaining reads were then used to generate *de novo* assemblies for each tissue type (with Trinity³⁴) which were filtered to remove erroneous contigs (see Technical Validation section). Protein coding regions in the assembled transcripts were then identified using TransDecoder (Trinity) (Dataset 5; Data Citation 1).

The resulting transcript sequences were functionally annotated using BLAST2GO^{35,36} against an in-house anuran database consisting of the Amphibia subset of the National Center for Biotechnology Information (NCBI; <http://www.ncbi.nlm.nih.gov>) non-redundant protein database. Functional annotation data from the Gene Ontology [GO] consortium, Enzyme Code and Inter Pro databases are contained in Dataset 6 [Data Citation 1]. The R package RSEM³⁷ was then used to quantify the abundance of genes and isoforms in individual frog tissue samples in combination with the above-described tissue-specific assembled transcriptomes, generating tables of transcript count data (Dataset 7; Data Citation 1).

Metabolomics methods

Metabolite isolation. The harvested tissue was transferred from methanol to a pre-chilled (dry ice) 2 ml cryo-tube. Each sample tube was then submerged in liquid nitrogen and the sample dried by lyophilisation in a LABCONCO Freezezone 2.5 Plus freeze-dryer (Labconco Corp., USA). The dried samples were homogenized by adding approximately 30 x 1.4 mm ceramic beads (Precellys, France) to each cryo-tube, followed by six 20 s rounds of vigorous agitation at 6,500 rpm in a Precellys 24 lysis cryo-mill (Bertin technologies, France). The metabolites were extracted by the addition of 500 µL of ice cold methanol to the homogenate, a further 20 s of vigorous agitation as already described, and 15 min mixing at 1,400 rpm at 4 °C in an Eppendorf Thermomixer (Eppendorf, USA). Cell debris were collected by centrifugation at 16,100 g for 30 min at 4 °C, and the supernatant containing metabolites transferred to a

fresh microcentrifuge tube. The extraction process was repeated three times with a second 500 μL of ice cold methanol, and finally using 300 μL of water. The supernatants were combined, and any remaining cell debris and/or precipitate collected by centrifuge as already described. The extracts were dried in preparation for derivatisation ahead of GC-MS analysis as described by Gummer, et al.³⁸. Briefly, this involved vacuum concentration of the metabolite extract, followed by dilution with 400 μL of LC-MS grade water, snap-freezing using liquid nitrogen and drying by lyophilisation. The entire volume of the skin-recovered metabolite extracts were dried, but only half of the recovered volume for the liver tissues (due to the larger sample weight). Additional metabolite extracts were set aside from surplus skin tissue to create a pooled extract, as later described.

Metabolite preparation and analysis. *Trimethylsilylation (TMS) derivatisation of metabolites for GC-MS analysis.* To ensure the amenability of metabolites to GC-MS analysis, the metabolites were derivatised by a combination of oximation (MEOX) and trimethylsilylation (TMS) as previously described³⁸. The metabolite lyophilisates were dissolved in 20 μL of pyridine (20 mg mL^{-1} methoxylamine HCl; Sigma-Aldrich) and incubated at 30 °C with agitation at 1,400 *r.p.m.* for two hours, followed by the addition of 40 μL N-Methyl-N-(trimethylsilyl) trifluoroacetamide (MSTFA; Sigma-Aldrich) and incubation at 37 °C with agitation at 650 *r.p.m.* for one hour. The derivatised metabolites were transferred to a 200 μL glass vial insert within a 1.5 mL glass amber vial. Five μL of hexane containing eight n-alkanes; n-decane, n-dodecane, n-pentadecane, n-nonadecane, n-docosane and n-octacosane at 6.25 $\mu\text{g mL}^{-1}$, and n-dotriacontane and n-hexatriacontane at 13.5 $\mu\text{g mL}^{-1}$, were added to each sample prior to GC-MS analysis.

GC-MS analysis of metabolites. Derivatised metabolites (1 μL) were analysed by GC-MS (Shimadzu QP2010 Ultra, Kyoto, Japan). The GC was equipped with an Agilent FactorFour VF-5 ms column (30 m x 0.25 mm x 0.25 μm +10 m EZ-Guard). The injection inlet temperature was 230 °C, with an interface temperature of 300 °C, and an ion source temperature of 230 °C. Helium was used as the carrier gas at a flow of between 0.8 and 1.0 mL min^{-1} . The inlet pressure was adjusted to elute mannitol (6-TMS) at 30.6 min. The temperature gradient consisted of an initial temperature of 70 °C, increasing at 1 °C per minute for 5 min before increasing to a final temperature of 320 °C at an oven ramp rate of 5.6 °C min^{-1} with a 10 min hold at maximum temperature. Ionisation was by electron ionization (EI) at 70 eV. The MS was operated in scan in the range m/z 40–600, at a scan rate of 5,600 amu sec^{-1} . For selected ion monitoring (SIM), ions were scanned at 0.38 s intervals.

Metabolite identification and processing. GC-MS data were acquired and analysed using GCMSsolution 2.61 (Shimadzu Corporation, Kyoto, Japan) and AnalyzerPro 2.7.0.0 (Spectral Works, Runcorn, UK). From a preliminary GC-MS analysis of skin and liver metabolites using a scan mode of acquisition, a selective ion monitoring (SIM) method was assembled using characteristic ions from a metabolite MS library and the preliminary data; and the remaining sample set analysed using a simultaneous full scan and SIM mode of acquisition. Chromatograms were deconvoluted by background subtraction of partially co-eluting ions. Relative analyte quantitation was achieved using a characteristic quantifier ion for each analyte [avoiding $\text{Si}(\text{CH}_3)_3$, m/z 73; characteristic of the silylation reaction]. Ions exceeding the upper dynamic concentration of the GC-MS were not used for quantitation, with lower abundant ions selected as alternative quantifier ions.

Metabolite identities were determined by mass spectral library search using the acquired scan data, using GCMSsolution 2.61 (Shimadzu Corporation, Kyoto, Japan) and AnalyzerPro 2.7.0.0 (Spectral Works, Runcorn, UK). The identities were assigned by comparison to authentic metabolite standards, requiring a similarity index of 80% or higher MS match and a retention index (RI) of ± 3 . The identification of metabolites without match to an available metabolite standard was sought from mass spectral similarity to an external MS library: Massbank, National Institute of Standards and Technology (NIST) or Wiley Registry™, and used for 'putative' metabolite assignments. An 'unknown' classification was assigned to metabolites that matched the mass spectra of a known metabolite class, with 70–80% similarity, but where the RI criteria did not match to that of the known metabolite standard. Metabolites without a match to known spectra were also deemed 'unknown' and named by the analytical characteristics using the prefix 'unknown', followed by the observed retention time (RT) and calculated RI. Metabolite accumulation data were normalised using the summed ion signal (total ion chromatogram) (Data Citation 3) (Dataset 9; Data Citation 1).

Data Records

For this study we deposited nine datasets. The first consists of animal signalment, survival and pathogen infection intensity data from the animals in Experiment A. These data are contained in Dataset 1, as a single comma-separated file (.csv format), entitled 'Dataset 1 Experiment A results data' (Data Citation 1). Each row below the header represents an individual frog ($n = 353$, from the original 355 minus two whose data were removed due to mortality pre-exposure), and columns ($n = 55$) contain frog identifier and treatment group information, signalment and measurement data, raw qPCR results, and length of survival data. Full descriptions of the column headers are contained in the associated readme file. Please see the associated metadata records in Supplementary File 1 for full details of study subjects and swab samples collected.

The second dataset consists of animal signalment and pathogen infection intensity data from the animals in Experiment B. These data are contained in Dataset 2, as a single comma-separated file (.csv format), entitled 'Dataset 2 Experiment B results data' (Data Citation 1). Each row below the header represents an individual frog ($n = 61$, from the original 51 frogs in this experiment plus the 10 frogs that were obtained from Experiment A and sampled when moribund at 28-30 days post exposure). Columns ($n = 27$) contain frog identifier and treatment group information, signalment and measurement data, and qPCR results data. Full descriptions of the column headers are contained in the associated readme file. Please see the associated metadata records in Supplementary File 1 for full details of study subjects and swab samples collected.

Dataset 3 consists of raw RNA-Seq reads from skin, liver and spleen tissues of each frog sampled as part of Experiment B ($n = 61$). Due to the multiple tissues sampled per frog (and a couple of poor quality samples that were excluded from library preparation) this dataset consists of 362 individual .fastq.gz files, comprising forward (R1) and reverse (R2) reads from paired-end Illumina Hi-Seq2000 sequencing for each of 60 liver, 61 skin, and 60 spleen tissue samples. These data have been submitted to the NCBI Sequence Read Archive and can be found under accession number: SRP096145 (Data Citation 2). Please see the associated metadata records in Supplementary File 1 for full details of study subjects and tissue samples collected.

The fourth dataset consists of a summary of the phred Q-score quality control data accompanying the sequence data from each tissue sample (described above). These data are contained in Dataset 4 as a single comma-separated file (.csv format) (Data Citation 1). Descriptions of the column headers are contained in the associated readme file.

The fifth dataset consists of the *de novo* assembled transcriptomes for each tissue type from frogs in Experiment B ($n = 61$). These data are contained in Dataset 5, as six individual .fasta text files, including both nucleotide sequence assembly files and amino acid sequence assembly files (translated using TransDecoder) for each of the three tissue types (skin, liver and spleen) (Data Citation 1). Descriptions of the sequence identifier lines are contained in the associated readme file.

The sixth dataset consists of functional annotation data (from the Gene Ontology [GO] consortium, Enzyme Code and Inter Pro databases) for each gene assembled, across the three tissue types (skin, liver and spleen). These data are contained in Dataset 6, as three individual comma-separated files (.csv format) (Data Citation 1). Full descriptions of the column headers are contained in the associated readme file.

The seventh dataset contains the raw gene/transcript counts data for each frog tissue sample (Experiment B, $n = 61$) resulting from allocation of sequence reads to genes from the transcriptome assemblies. These data are contained in Dataset 7, as 12 individual tab-separated text files (.txt) and comma-separated files (.csv) (Data Citation 1). The four files for each tissue type (skin, liver and spleen) represent raw (1) counts, (2) TMM.EXPR files, (3) TPM.not_cross_norm files, and (4) normalisation information (as per the standard output from RSEM). The first row of these files (1-3 above) represents frog ID, and the first element of all subsequent rows represents transcript/isoform ID.

The eighth and ninth datasets contain the metabolite accumulation data from skin and liver tissues for each frog from Experiment B ($n = 61$). These data have been scaled by dividing by the summed ion signal (total ion chromatogram). Dataset 8 has been submitted to the MetaboLights data repository (Data Citation 3). An alternative presentation of this data is also contained as a single comma-separated file (.csv format) (Dataset 9; Data Citation 1), with full descriptions of the column headers (and associated analyte data) contained in the associated readme file. Please see the associated metadata records in Supplementary File 1 for full details of study subjects and tissue samples collected for the metabolomics work.

Technical Validation

Quality control of the frog exposure experiment

Blinded, controlled and stratified randomized design of the frog exposure experiment. We controlled for technical confounding and potential batch effects *a priori* in our experimental design using a variety of standard techniques including (1) blinding operators to treatment groups, (2) including sham-exposed negative control treatment groups of frogs, and (3) employing a stratified random design. At the commencement of the pre-experimental acclimation period, frogs were assigned a unique ID number (e.g. Lva018) that was randomized with respect to source population and clutch and distributed randomly among frogs from Experiments A and B. Frogs were then assigned to treatment groups (including control groups) and prospective sampling periods randomly using a stratified block design (ie, frogs were chosen randomly from among source population and clutch groups up to a total number determined *a priori* for each treatment).

Physical layout of the frog exposure experiment. Frogs in the exposure experiments were physically placed according to their randomized ID number in rows on treatment shelves, whereby individuals from different clutches, populations, treatments and sampling dates were placed randomly with respect to each other. Both Experiment A and B were run concurrently under identical environmentally-controlled quarantine conditions inside an air-conditioned laboratory with artificial light source and filtered water source.

Controlling for potential batch effects due to date of sampling period. In order to control and test for potential batch effects that might be introduced through the multiple sampling dates utilized for Experiment B (for example, associated with differences in environment or technique, or improved efficiency with repeated sampling through time), at each of the three subclinical sampling sessions (4, 8, and 14 days post exposure), we additionally sampled sham-exposed negative control individuals from each population (from the stratified random design). The sample results from these individuals were then able to be compared between sampling sessions to identify batch effects.

Quality control of the transcriptomics study

Total RNA extraction protocol quality control. The extraction of total RNA from frog tissue samples was performed with standard kits using manufacturer protocols according to frog ID number within tissue type. That is, over several days, all liver samples were processed, following frog ID, then all skin samples were processed likewise, followed by all spleen samples. We acknowledge that as a logistical necessity, different brand kits were used to extract total RNA from skin/liver samples as opposed to spleen samples, however this should not impact resulting analyses because the results are analyzed in a tissue-specific manner (and data from different tissues were not intended to be compared due to the vastly different gene expression profiles expected).

Total RNA sample quality and quantity measures. All resulting total RNA samples were subject to rigorous quality control prior to library preparation, including (1) analysis of RNA concentration, 260/280 (~ 2.0) and 260/230 (2.0-2.2) absorption ratios via Nanodrop 1000 spectrophotometer, (2) quantification using a fluorimetric Quant-iT RiboGreen RNA assay, and (3) quality assessment using capillary electrophoresis (Agilent Caliper LabChip GX high-throughput BioAnalyzer). To pass quality control samples had to have > 1 µg, and the RNA Integrity Number (RIN) > 8. In-house results for each sample from the Nanodrop 1000 spectrophotometer are included in the associated metadata record.

Quality controls during sequencing. Multiplexing and sequencing via Illumina HiSeq-2000 platform were performed following standard protocols with PhiX Control v3 internal control spiked at 1% into every lane of each flow cell (as recommended by the manufacturer), by the University of Minnesota's BioMedical Genomics Centre (now known as University of Minnesota Genomics Center (UMGC); <http://genomics.umn.edu/>). Samples were multiplexed into flow cell lanes by tissue type.

FastQC for assessing sequenced read quality. Read sequence data from each sample were examined for base-call quality using standard software for the purpose, FastQC (www.bioinformatics.babraham.ac.uk/projects/fastqc/). Summaries of the Q-score quality control data accompanying the sequence data from each tissue sample are contained in Dataset 4 (Data Citation 1), with descriptions of the column titles contained in the associated readme file.

De novo transcriptome assembly quality assessment. To reduce the number of partial or erroneous contigs during transcriptome assembly we used the 'align and estimate abundance.pl' script from the Trinity package³⁴, to map reads back to the assembly. All contigs with fewer than four reads per million mappable reads were discarded, as previously described^{39,40}. Trinity toolkit utilities were then used to assess the quality of resulting transcriptomes. The N50 contig lengths were 2531, 2433, and 2258 bases for liver, skin and spleen assemblies respectively. Similarly, the total number of Trinity 'genes' assembled were 21269, 26894, and 28876 for liver, skin and spleen assemblies respectively. The RNA-Seq read representation of our tissue-specific transcriptome assemblies were above the optimal threshold (80%) for proper read pairs (skin 85.24%, liver 89.68% and spleen 83.43%). When considering the representation of protein-coding genes in the assemblies, 65% of skin, 70% of liver and 58% of spleen sequences with BLAST matches had 80% alignment coverage.

Functional annotation quality control. The functional annotation software suite BLAST2GO³⁶ uses standard algorithms (including the basic linear alignment search tool [BLAST]), as well as quality measures to obtain most parsimonious functional gene annotations. The three most useful measures are (1) the minimum Expect value (E-value), (2) the mean sequence similarity, and (3) consideration of sequence length. In order to exclude 'chance' annotations, we employed the commonly accepted thresholds of retaining annotations with a minimum E-value of < 1x10⁻⁴ and mean sequence similarity > 60%. These data (and further explanations of these measures) can be found in Dataset 6 (Data Citation 1).

Testing for potential batch effects of tissue sampling date on RNA-seq results. In an accompanying study examining differential gene expression²¹ we compared the numbers of differentially expressed genes shared between unexposed control frogs (pooled between populations) sampled at different dates (4, 8 and 14 DPE). Our results demonstrated that there was no evidence for a sampling time batch effect in either the skin or spleen samples, but there was evidence for a mild batch effect in the liver samples (158 genes were significantly differentially expressed between the four and eight day post exposure sampling groups, in both the infected and controls). This difference may have been attributable to relatively rapid liver autolysis compared with the other two tissues sampled (livers were also last to be

sampled during necropsy), and a mildly increased sampling time taken during the first sampling session. In the same study²¹ we compared gene expression levels between negative control (uninfected) and exposed (infected) frog groups and as expected, found distinct clustering by population for all three tissue types using multi-dimensional scaling plots (Fig. 3, reprinted with permission from Grogan et al. 2018²¹).

Quality control of the metabolomics study

Exogenous analytical standards for quality control. To allow the collection of retention-time aligned data, consistent with the metabolite reference MS-library, the GC inlet pressure was adjusted prior to sample analysis to elute a mannitol (D-mannitol, 6TMS) external reference standard at a retention time of 30.6 min, and the ¹³C-sorbitol (¹³C-sorbitol, 6TMS) internal reference standard at 30.7 min. Prior to GC-MS acquisition, to each sample was added five microliters of hexane containing a mixture of eight n-alkane retention index reference standards, to allow retention index (RI) calculation. A RI was calculated for each analyte measurement relative to the RI of each of the eight n-alkanes. Metabolite identities were assigned by comparison to a MS-library of authentic metabolite standards analysed under the same analytical conditions, with the RT of mannitol (6TMS) fixed as described, and metabolite match criteria requiring a RI of ± 3 (Data Citation 3), (Dataset 9; Data Citation 1).

Supportive data for metabolite identification. Metabolite identities were assigned by comparison to a MS-library of authentic metabolite standards, as already described. Where an additional confirmation of metabolite identity was sought, for example in the identification of serotonin (for which the mass spectrum is predominantly dominated by a single ion, m/z 174, together with the TMS-derivatives of other biogenic amines), pooled replicates of the metabolite extracts were set aside for verification of metabolite identification by ‘spiking’ with a series of metabolite standards, prior to GC-MS analysis. Identity was confirmed by a corresponding increase in intensity of the respective formerly observed ion(s) within the mass spectra. A single reference pool of metabolite extract was divided into six aliquots. Prior to drying, 65 μl of 25 $\mu\text{g mL}^{-1}$ of a series of metabolite reference standards (in 50% methanol) was added to three replicates, and 65 μl of 50% methanol was added to another three replicate tubes for comparison. Each was dried in preparation for GC-MS analysis.

Exclusion of analytical artifacts. Analytical artifacts were determined by analysis of blank extraction controls (containing no tissue sample). Analytes observed within these analyses were removed from the metabolite measurement data, as they were deemed of non-biological origin and thus not metabolites. Analytes suspected of being analytical artefacts (by MS-library match) but not confirmed by the extraction controls were not removed from the final data matrix (marked as likely artifacts within Dataset 9).

Testing for potential instrumental batch effects on metabolomics results. In an accompanying study examining differential metabolite accumulation (L. Grogan unpublished data) we compared the sum of metabolite concentrations between metabolite extraction dates and found mild instrumental batch effects in the skin tissue samples, consistent with preventative GC-MS maintenance regimens (Fig. 4).

References

1. Stuart, S. N. *et al.* Status and trends of amphibian declines and extinctions worldwide. *Science* **306**, 1783–1786 (2004).
2. Berger, L. *et al.* Chytridiomycosis causes amphibian mortality associated with population declines in the rain forests of Australia and Central America. *Proc Natl Acad Sci USA* **95**, 9031–9036 (1998).
3. Olson, D. H. *et al.* Mapping the global emergence of *Batrachochytrium dendrobatidis*, the amphibian chytrid fungus. *PLoS ONE* **8**, 13 (2013).
4. Skerratt, L. F. *et al.* Spread of chytridiomycosis has caused the rapid global decline and extinction of frogs. *EcoHealth* **4**, 125–134 (2007).
5. Scheele, B. C. *et al.* Interventions for reducing extinction risk in chytridiomycosis-threatened amphibians. *Conserv. Biol.* **28**, 1195–1205 (2014).
6. Scheele, B. C. *et al.* After the epidemic: Ongoing declines, stabilizations and recoveries in amphibians afflicted by chytridiomycosis. *Biol. Conserv.* **206**, 37–46 (2017).
7. Skerratt, L. F. *et al.* Priorities for management of chytridiomycosis in Australia: saving frogs from extinction. *Wildl. Res* **43**, 105–120 (2016).
8. Bonneaud, C. *et al.* Rapid evolution of disease resistance is accompanied by functional changes in gene expression in a wild bird. *Proc. Natl. Acad. Sci. USA* **108**, 7866–7871 (2011).
9. Bonneaud, C., Balenger, S. L., Zhang, J. W., Edwards, S. V. & Hill, G. E. Innate immunity and the evolution of resistance to an emerging infectious disease in a wild bird. *Mol. Ecol.* **21**, 2628–2639 (2012).
10. Ragimekula, N. *et al.* Marker assisted selection in disease resistance breeding. *Journal of Plant Breeding and Genetics* **1**, 90–109 (2013).
11. Miedaner, T. & Korzun, V. Marker-Assisted Selection for disease resistance in wheat and barley breeding. *Phytopathology* **102**, 560–566 (2012).
12. Savage, A. E. & Zamudio, K. R. MHC genotypes associate with resistance to a frog-killing fungus. *Proc. Natl. Acad. Sci. USA* **108**, 16705–16710 (2011).
13. Scheele, B. C. *et al.* High adult mortality in disease-challenged frog populations increases vulnerability to drought. *Journal of Animal Ecology* **85**, 1453–1460 (2016).
14. Osborne, W., Hunter, D., Hollis, G. in *Declines and disappearances of Australian frogs* (ed. Campbell A.) 145–157 (Environment Australia, 1999).
15. Scheele, B. C., Hunter, D. A., Skerratt, L. F., Brannelly, L. A. & Driscoll, D. A. Low impact of chytridiomycosis on frog recruitment enables persistence in refuges despite high adult mortality. *Biol. Conserv.* **182**, 36–43 (2015).

16. Bataille, A. *et al.* Susceptibility of amphibians to chytridiomycosis is associated with MHC class II conformation. *Proc. R. Soc. B-Biol. Sci* **282**, 9 (2015).
17. Brannelly, L. A., Berger, L. & Skerratt, L. F. Comparison of three widely used marking techniques for adult anuran species *Litoria verreauxii alpina*. *Herpetol. Conserv. Biol.* **9**, 428–435 (2014).
18. Brannelly, L. A. *et al.* Dynamics of Chytridiomycosis during the Breeding Season in an Australian Alpine Amphibian. *PLoS One* **10**, 15 (2015).
19. Brannelly, L. A. *et al.* Chytrid infection and post-release fitness in the reintroduction of an endangered alpine tree frog. *Anim. Conserv.* **19**, 153–162 (2016).
20. Brannelly, L. A., Webb, R. J., Skerratt, L. F. & Berger, L. Effects of chytridiomycosis on hematopoietic tissue in the spleen, kidney and bone marrow in three diverse amphibian species. *Pathog. Dis* **74**, 10 (2016).
21. Grogan, L. F. *et al.* Evolution of resistance to chytridiomycosis is associated with a robust early immune response. *Mol. Ecol.* In press doi:10.1111/MEC.14493 (2018).
22. Farrer, R. A. *et al.* Multiple emergences of genetically diverse amphibian-infecting chytrids include a globalized hypervirulent recombinant lineage. *Proc. Natl. Acad. Sci. USA* **108**, 18732–18736 (2011).
23. Cashins, S. D. *et al.* Prior infection does not improve survival against the amphibian disease chytridiomycosis. *PLoS ONE* **8**, 7 (2013).
24. Berger, L., Speare, R. & Skerratt, L. F. Distribution of *Batrachochytrium dendrobatidis* and pathology in the skin of green tree frogs *Litoria caerulea* with severe chytridiomycosis. *Dis. Aquat. Org* **68**, 65–70 (2005).
25. Colombo, B. M., Scalvenzi, T., Benlamara, S. & Pollet, N. Microbiota and mucosal immunity in amphibians. *Front. Immunol* **6**, 15 (2015).
26. Jenne, C. N. & Kubes, P. Immune surveillance by the liver. *Nat. Immunol.* **14**, 996–1006 (2013).
27. Garland, S., Baker, A., Phillott, A. D. & Skerratt, L. F. BSA reduces inhibition in a TaqMan (R) assay for the detection of *Batrachochytrium dendrobatidis*. *Dis. Aquat. Org* **92**, 113–116 (2009).
28. Hyatt, A. D. *et al.* Diagnostic assays and sampling protocols for the detection of *Batrachochytrium dendrobatidis*. *Dis. Aquat. Org* **73**, 175–192 (2007).
29. Skerratt, L. F. *et al.* Validation of diagnostic tests in wildlife: the case of chytridiomycosis in wild amphibians. *J. Herpetol.* **45**, 444–450 (2011).
30. Bolger, A. M., Lohse, M. & Usadel, B. Trimmomatic: a flexible trimmer for Illumina sequence data. *Bioinformatics* **30**, 2114–2120 (2014).
31. Hansen, K. D., Brenner, S. E. & Dudoit, S. Biases in Illumina transcriptome sequencing caused by random hexamer priming. *Nucleic Acids Res.* **38**, 7 (2010).
32. Brown, C. T., Howe, A., Zhang, Q., Pyrkosz, A. B. & Brom, T. H. A reference-free algorithm for computational normalization of shotgun sequencing data. *arXiv e-print*, 1203.4802v1202 [q-bio.GN] (2012).
33. Langmead, B., Trapnell, C., Pop, M. & Salzberg, S. L. Ultrafast and memory-efficient alignment of short DNA sequences to the human genome. *Genome Biol.* **10**, 10 (2009).
34. Haas, B. J. *et al.* De novo transcript sequence reconstruction from RNA-seq using the Trinity platform for reference generation and analysis. *Nat. Protoc.* **8**, 1494–1512 (2013).
35. Conesa, A. *et al.* Blast2GO: a universal tool for annotation, visualization and analysis in functional genomics research. *Bioinformatics* **21**, 3674–3676 (2005).
36. Gotz, S. *et al.* High-throughput functional annotation and data mining with the Blast2GO suite. *Nucleic Acids Res.* **36**, 3420–3435 (2008).
37. Li, B. & Dewey, C. N. RSEM: accurate transcript quantification from RNA-Seq data with or without a reference genome. *BMC Bioinformatics* **12**, 16 (2011).
38. Gummer, J. P. A., Trengove, R. D., Oliver, R. P. & Solomon, P. S. Dissecting the role of G-protein signalling in primary metabolism in the wheat pathogen *Stagonospora nodorum*. *Microbiology-(UK)* **159**, 1972–1985 (2013).
39. Moghadam, H. K., Harrison, P. W., Zachar, G., Székely, T. & Mank, J. E. The plover neurotranscriptome assembly: Transcriptomic analysis in an ecological model species without a reference genome. *Mol. Ecol. Resour.* **13**, 696–705 (2013).
40. Harrison, P. W., Mank, J. E. & Wedell, N. Incomplete sex chromosome dosage compensation in the indian meal moth, plodia interpunctella, based on de novo transcriptome assembly. *Genome Biology and Evolution* **4**, 1118–1126 (2012).
41. Hallgren, W. *et al.* The Biodiversity and Climate Change Virtual Laboratory: Where ecology meets big data. *Environmental Modelling & Software* **76**, 182–186 (2016).
42. Smith, M. J., Osborne, W. & Hunter, D. Geographic variation in the advertisement call structure of *Litoria verreauxii* (Anura: Hylidae). *Copeia* 750–758 (2003).
43. Merow, C., Smith, M. J. & Silander, J. A. A practical guide to MaxEnt for modeling species' distributions: what it does, and why inputs and settings matter. *Ecography* **36**, 1058–1069 (2013).
44. Phillips, S. J., Anderson, R. P. & Schapire, R. E. Maximum entropy modeling of species geographic distributions. *Ecological Modelling* **190**, 231–259 (2006).
45. Belbin, L. & Williams, K. J. Towards a national bio-environmental data facility: experiences from the Atlas of Living Australia. *International Journal of Geographical Information Science* **30**, 108–125 (2016).

Data Citations

1. Grogan, L. F. *et al.* *Dryad Digital Repository* <https://doi.org/10.5061/dryad.t1p7c> (2018).
2. NCBI Sequence Read Archive SRP096145 (2018).
3. Gummer, J. & Grogan, L. *MetaboLights* MTBLS457 (2018).

Acknowledgements

We thank E. Rosenblum and L. Rollins-Smith for advice on study design, and R. Speare for initiating this collaboration. We thank volunteers at Taronga Zoo (B. Keraunos and L. Powe), R. Spindler, K. Rose and members of the Taronga Conservation Society Herpetofauna Department for assistance with logistics for the clinical experiment and species' insights. We thank S. Bell and R. Webb for assistance with qPCR analyses. We also thank C. Rawlinson and H. Wong for valuable technical assistance towards GC-MS analyses. This study was conducted with approval by the James Cook University Animal Ethics Committee (Certificate no. A1589), the Taronga Conservation Society Australia Animal Ethics Committee (4c/01/10) and Scientific License number: S12848 (D. Hunter). The various components of this work were funded by the Australian Research Council, Australian Biosecurity Cooperative Research Centre for Emerging Infectious Diseases, Morris Animal Foundation, Taronga Conservation Society, New

South Wales Office of Environment and Heritage, US Fish and Wildlife Service – Wildlife Without Borders program and the IUCN Amphibian Specialist Group Seed Grants program. L.F.G. and L.B. were supported by Australian Research Council grants FT100100375, DP120100811, LP110200240 and the Taronga Conservation Science Initiative. Metabolomics Australia is a Bioplatforms Australia (BPA) funded initiative. J.P.A.G. was supported through BPA. The funders had no role in study design, data collection and analysis, decision to publish, or preparation of the manuscript.

Author Contributions

L.F.G. conceived the research, conducted the clinical experiment and collected samples, conducted RNA extractions, conducted bioinformatics analyses, curated the data files, and wrote the manuscript. J.M. conducted bioinformatics analyses, curated the data files, and edited the manuscript. J.P.A.G. conducted metabolomics analyses, curated the data files, and edited the manuscript. B.C.S. provided contextual field knowledge and expertise, and edited the manuscript. L.B. conceived the research, and edited the manuscript. S.D.C. conceived the research, conducted the clinical experiment, and collected samples. M.S.M. provided advice and assistance with the captive husbandry components, and edited the manuscript. P.H. provided advice and assistance with the captive husbandry components, and edited the manuscript. D.A.H. provided contextual field knowledge and expertise, and edited the manuscript. R.D.T. conducted metabolomics analyses, and edited the manuscript. L.F.S. conceived the research, and edited the manuscript.

Additional information

Table 3 is available only in the online version of this paper.

Competing interests: The authors declare no competing interests.

How to cite: Grogan, L. F. *et al.* Survival, gene and metabolite responses of *Litoria verreauxii alpina* frogs to fungal disease chytridiomycosis. *Sci. Data* 5:180033 doi: 10.1038/sdata.2018.33 (2018).

Publisher's note: Springer Nature remains neutral with regard to jurisdictional claims in published maps and institutional affiliations.



Open Access This article is licensed under a Creative Commons Attribution 4.0 International License, which permits use, sharing, adaptation, distribution and reproduction in any medium or format, as long as you give appropriate credit to the original author(s) and the source, provide a link to the Creative Commons license, and indicate if changes were made. The images or other third party material in this article are included in the article's Creative Commons license, unless indicated otherwise in a credit line to the material. If material is not included in the article's Creative Commons license and your intended use is not permitted by statutory regulation or exceeds the permitted use, you will need to obtain permission directly from the copyright holder. To view a copy of this license, visit <http://creativecommons.org/licenses/by/4.0/>

The Creative Commons Public Domain Dedication waiver <http://creativecommons.org/publicdomain/zero/1.0/> applies to the metadata files made available in this article.

© The Author(s) 2018